Group A *Streptococcus* Induces Lysosomal Dysfunction in THP-1 Macrophages

Scott T. Nishioka[1†], Joshua Snipper[1†], Jimin Lee[1], Joshua Schapiro[1], Robert Z. Zhang[1], Hyewon Abe[1], Andreas Till[2,3], Cheryl Y.M. Okumura[1]*

[1]Biology Department, Occidental College, Los Angeles, CA 90041, USA

[2]Division of Biological Sciences and The San Diego Center for Systems Biology, University of California San Diego, La Jolla, CA 92093-0688, USA

[3]University Hospital of Bonn, Bonn, Germany

[†]These authors have contributed equally to this work and share first authorship

*** Correspondence:**
Cheryl Okumura
okumura@oxy.edu

Keywords: Group A *Streptococcus*, streptolysin O (SLO), macrophage, lysosome, vacuolar ATPase, cathepsin B

Abstract

The human-specific bacterial pathogen Group A *Streptococcus* (GAS) is a significant cause of morbidity and mortality. Macrophages are important to control GAS infection, but previous data indicate that GAS can persist in macrophages. In this study, we detail the molecular mechanisms by which GAS survives in THP-1 macrophages. Our fluorescence microscopy studies demonstrate that GAS are readily phagocytosed by macrophages, but persist within phagolysosomes. These phagolysosomes are not acidified, which is in agreement with our findings that GAS cannot survive in low pH environments. We find that the secreted pore-forming toxin Streptolysin O (SLO) perforates the phagolysosomal membrane, allowing leakage of not only protons, but large proteins including the lysosomal protease cathepsin B. Additionally, GAS blocks the activity of vacuolar ATPase (v-ATPase) to prevent acidification of the phagolysosome. Thus, while GAS does not inhibit fusion of the lysosome with the phagosome, it has multiple mechanisms to prevent proper phagolysosome function, allowing for persistence of the bacteria within the macrophage. This has important implications for not only the initial response but the overall functionality of the macrophages, which may lead to the resulting pathologies in GAS infection. Our data suggests that therapies aimed at improving macrophage function may positively impact patient outcomes in GAS infection.

Word count: Abstract: 204; Manuscript: 5642 (omitting references and figure legends); Number of figures: 5

1 Introduction

GAS is a significant cause of morbidity and mortality worldwide, but especially in medically underserved areas where antibiotic therapy may not be promptly available . Infection produces wide-ranging clinical manifestations including pharyngitis, acute rheumatic fever (ARF) often leading to rheumatic heart disease, and invasive disease such as necrotizing fasciitis (1). Acting as the first line

of defense against such infections, macrophages are critical for the early control and resolution of GAS infection (2,3). However, GAS has been shown to survive intracellularly in macrophages during both acute invasive soft tissue infection and asymptomatic carriage (3–5). Although GAS remains highly sensitive to beta-lactam antibiotics, the gold standard of treatment (6), the ability of bacteria to persist in macrophages and re-emerge after antibiotic treatment poses a therapeutic challenge (4).

As both phagocytes and antigen-presenting cells, macrophages function at the intersection of innate and adaptive immunity and are therefore critical for identifying and defending against infection. Macrophages engulf bacterial pathogens into phagosomes, which fuse with lysosomes that deliver proteolytic enzymes to facilitate bacterial destruction. These enzymes have optimal proteolytic activity under acidic conditions, and therefore lysosomal acidification is important for macrophage bactericidal function and subsequent antigen presentation (8). Inhibition of either lysosomal fusion with bacteria-containing phagosomes or phagolysosomal acidification is an evasion tactic employed by several bacterial pathogens including *Mycobacterium tuberculosis*, *Legionella pneumophila*, and *Staphylococcus aureus* (8–10). GAS may employ similar tactics to survive intracellularly within macrophages and to evade the adaptive immune response upon host re-infection, which may contribute to the development of pathologies such as toxic shock syndrome (11).

GAS is a human-specific pathogen and has evolved mechanisms to survive the immune response (12). Previous data have indicated that phagocytosed GAS can prevent fusion with destructive organelles such as azurophilic granules and lysosomes (13,14). Other reports have shown that while GAS-containing phagosomes do fuse with lysosomes, GAS survives within macrophages via the secretion of virulence factors such as Streptolysin O (SLO) and NADase (15,16). SLO is a cholesterol-dependent cytolysin that oligomerizes to form large pores (~30 nm) within the host cell membrane (17) that allows the loss of proteins up to 15nm in diameter (18). As a result, SLO is hypothesized to permeabilize the phagolysosomal membrane, permitting free flow of protons out of the phagolysosome and limiting the activity of lysosomal proteases that facilitate intracellular killing (16,19). Interestingly, it has also been reported that GAS is capable of preventing lysosomal acidification by preventing the recruitment of the vacuolar ATPase (v-ATPase) (20). In the context of these data, it is unclear what mechanisms are contributing to GAS intracellular survival in macrophages. In this paper, we used the human monocytic cell line THP-1 differentiated into macrophages to understand the molecular mechanism by which GAS survives in macrophages. We find that not only does GAS induce leakage of large proteins from the phagolysosome into the cytosol, but that acidification of the phagolysosome is also limited. This has important consequences for the survival of the bacteria within the macrophage and underscores the need to mount a proper macrophage response in GAS infection to improve patient outcomes.

2 Materials and Methods

2.1 Antibodies and chemicals

Antibodies to the following proteins were used in this study: EEA-1 (Abcam, ab2900), LAMP-2 (Abcam, ab25631), V_0D_1 (Abcam, ab56441), Cathepsin B (Cell Signaling Technology, D1C7Y), LAMP-1 (Cell Signaling Technology, #9091), V_1A (Abnova, H00000523-A01), and beta-actin (Thermo Fisher Scientific, MA5-15739). Fluorescent secondary antibodies were purchased from Thermo Fisher Scientific. The following fluorescent probes were purchased from Thermo Fisher Scientific: Alexa Fluor 488 Hydrazide (A10436), Oregon Green 488 Anionic, Lysine Fixable Dextran,10,000 MW (D7171) and 70,000 MW (D7173), and LysoTracker DeepRed (L12492).

83 40,000 and 70,000 MW Fluorescein isothiocyanate (FITC) dextrans were purchased from Millipore
84 Sigma. To generate antibody-coupled beads, 0.1um Carboxylate-Modified Microspheres (Thermo
85 Fisher Scientific) were coupled to approximately 400mg normal pooled human serum (Thermo
86 Fisher Scientific) using 2% 1-Ethyl-3-(3-dimethylaminopropyl) carbodiimide hydrochloride
87 (QBiosciences). The reaction was quenched with 40mM ethanolamine and resuspended in PBS.
88 Successful coupling of the beads was assessed by fluorescence microscopy showing increased
89 phagocytosis by THP-1 macrophages compared with uncoupled beads (data not shown). 1mM L-
90 leucyl L-leucine O-methyl ester (LLOMe, Cayman Chemical, #16008) was incubated with cells to
91 induce lysosomal damage.

92 **2.2 Bacterial strains**

93 Wild-type (WT) GAS strain M1T1 5448 (M1 GAS) was originally isolated from a patient with
94 necrotizing fasciitis and toxic shock syndrome (21). Isogenic mutant strains lacking Streptolysin O
95 (ΔSLO), Streptolysin S (via lack of SagA, ΔSagA) and Emm1 (ΔM1) were previously described (22–
96 24). Bacterial strains were cultivated in Todd-Hewitt broth (THB) at 37˚C. For all experiments,
97 bacteria were grown to log phase in the presence of 1:200 pooled normal human serum (Thermo
98 Fisher Scientific) to opsonize bacteria. The gene for monomeric WASABI (mWASABI) (7,25) was
99 codon-optimized for expression in bacteria and synthesized in a shuttle vector (GenScript; see
100 supplemental data for amino acid sequence). The gene was subcloned into pDCerm (26) and the
101 resulting plasmid (pWASABI) was transformed into WT M1 GAS and the ΔSLO mutant. Plasmid-
102 bearing strains were maintained in THB supplemented with 5ug/mL erythromycin. Heat-killed (HK)
103 bacteria were prepared by incubating a known concentration of bacteria at 95°C for 10 min. followed
104 by a 15 min. opsonization in 1:200 pooled normal human serum at room temperature.

105 **2.3 Cell Culture**

106 THP-1 cells were purchased from Sigma (cat. 88081201) and cultured in RPMI supplemented with
107 10% heat inactivated fetal bovine serum (FBS) (Corning), 2mM L-glutamine and 100 U/mL
108 penicillin/100 µg/mL streptomycin at 37°C/5% CO_2. Cells were differentiated to macrophages using
109 20nM phorbol 12-myristate 13-acetate (PMA) (MilliporeSigma) 24-48 hours prior to experiments.

110 **2.4 Immunofluorescence**

111 2.5 x 10^5 THP-1 cells were seeded on coverslips in the presence of 20nM PMA 24-48 hours prior to
112 experiments. For dextran leakage assays, cells were incubated in media containing 20ug/mL of the
113 indicated dextran or 500ug/mL 70kD dextran overnight, washed and chased in cell culture media for
114 2 hours prior to bacterial infection. For infection experiments with two rounds of infection, secondary
115 infection bacteria were labeled with 10uM CellTracker Orange (Thermo Fisher Scientific) 30 min.
116 prior to infection. Bacteria were combined with cells at an MOI = 10 in RPMI supplemented with 2%
117 FBS only (no antibiotics) and plates were centrifuged at 500 x g to synchronize bacterial contact with
118 cells. At the indicated time points, cells were fixed with 4% paraformaldehyde or 3.7% formaldehyde
119 for 10 min. at room temperature. Cells were incubated with blocking solution (10% goat serum, 3%
120 BSA and 0.1% Triton X-100 in PBS), then incubated with the indicated primary antibodies for 1 hour
121 at room temperature in block solution. Cells were washed and incubated with the indicated secondary
122 antibodies for 1 hour at room temperature. GAS opsonized in human serum were detected using
123 fluorescent anti-human IgG antibodies where indicated. Cells were washed and mounted onto slides
124 with ProLong antifade reagent with DAPI (Thermo Fisher Scientific). Slides were imaged on an
125 inverted Leica TCS SP5 confocal microscope using a 63x/1.40 oil objective with 2-3x digital zoom at
126 calibrated magnifications and recorded with LAS AF software (Leica). Quantitation of dextran and

127 LAMP-1 colocalization with bacteria was analyzed with CellProfiler 3.1.9 (27) using the Otsu
128 thresholding method and the MeasureImageOverlap module. To automatically count bacteria and
129 cells, either fluorescence (bacteria) or brightfield (THP-1 macrophages) images were thresholded,
130 objects were filled and average object size was used to count cells. For LAMP-1, colocalization is
131 expressed as the percentage of GAS fluorescence that colocalized with LAMP-1 fluorescence, and
132 the number of bacteria per cell was estimated by dividing the total number of bacteria by the total
133 number of cells counted in each image. For dextran staining, colocalization is expressed as the
134 percentage of dextran fluorescence that colocalized with GAS fluorescence. For quantitation of
135 mWASABI-expressing bacteria within phagosomes, images were coded and counted manually in a
136 blind fashion by at least 3 independent reviewers. For manually counted cells, the number of bacteria
137 per cell and the number of infected cells was calculated by averaging the number of bacteria in
138 infected cells across all counted images within an experiment. For all imaging data, at least 3
139 independent experiments were performed, at least 16 images containing >10 cells per image were
140 analyzed and >100 cells were counted per time point.

141 **2.5 Verification of pH sensitivity of mWASABI in GAS**

142 To assess the fluorescence intensity of mWASABI in live GAS, log phase cultures of bacteria were
143 incubated on coverslips in THB with 10mM HEPES adjusted to the indicated pH for 1 hour at 37°C.
144 Bacteria were fixed with 2% paraformaldehyde and analyzed by confocal microscopy. Gain settings
145 were adjusted to bacteria incubated in pH 7 media, and the settings were applied to all other
146 conditions. Images were thresholded and the corrected total cell fluorescence (integrated density –
147 average background integrated density) of each bacterial cell was measured using ImageJ.

148 **2.6 Acidification assay**

149 10^5 THP-1 cells were seeded with 20nM PMA in 96-well black plates with clear bottoms overnight.
150 The following day, cells were fed 500ug/mL 70kD FITC-dextran overnight. On the third day, cells
151 were chased with normal cell culture media (RPM1 supplemented with 10% FBS, no antibiotics) for
152 2 hours prior to infection. Cells were infected at an MOI of 10 with either the indicated bacterial
153 strain or Ab-conjugated latex beads in RPMI supplemented with 2% FBS only (no antibiotics) and
154 plates were centrifuged at 500 x g to synchronize bacterial contact with cells. Fluorescence intensity
155 at 480nm/535nm (Em/Ex) was monitored at 37°C in a fluorescent plate reader for 3 hours.

156 **2.7 Bacterial survival in different pH media**

157 Bacteria were incubated in THB with 10mM HEPES adjusted to the indicated pH. For bacterial
158 growth, cultures were adjusted to an OD_{600nm} of 0.1 and incubated at 37°C. OD_{600nm} was measured
159 every 15 min. For bacterial survival, 2 x 10^5 cfu log phase bacteria were added to 250ul pH-adjusted
160 culture media in 96 well plates. At the indicated time point, a 25ul aliquot was removed from the
161 culture and quantitated by plating on agar plates.

162 **2.8 Cell fractionation and Western blot**

163 Following a 30 min. infection period, a total of 10^7 PMA-differentiated cells were scraped and
164 collected in 1 mL of fractionation buffer (50 mM KCl, 90 mM K-Gluconate, 1 mM EGTA, 5 mM
165 MgCl2, 50 mM sucrose, 20 mM HEPES, pH 7.4, 5 mM glucose, 1X HALT phosphatase/protease
166 inhibitor cocktail (Thermo Fisher Scientific), 1ug/mL pepstatin (Millipore Sigma), and 1mM PMSF
167 (Millipore Sigma)). Cells were lysed by nitrogen cavitation equilibrated on ice for 30 min. at 400 psi.
168 The resulting lysates were fractionated into membrane and cytosolic fractions by centrifugation at

169 16,000 x g at 4˚C for 15 min. (pellet = membrane fraction, supernatant = cytosolic fraction). Protein
170 concentrations were measured by BCA assay (Thermo Fisher Scientific). 10ug of each sample was
171 run on SDS-PAGE gels and transferred to a 0.2um PVDF membrane. Blots were blocked with 5%
172 (w/v) non-fat dry milk in 1X Tris-buffered saline with 0.1% Tween 20 (TBST). Blots were probed
173 with the indicated antibodies overnight at 4˚C. Relative protein concentrations were quantified by
174 densitometry analysis in ImageLab v. 6.0.1 (BioRad). v-ATPase assembly was measured by
175 normalizing V_1A densitometry values in the membrane fraction to the V_0D_1 loading controls in
176 membrane fractions and calculating the ratio of V_1A in the sample compared with uninfected
177 macrophages (28).

178 **2.9 Cathepsin B activity assay**

179 4 x 10^6 PMA-differentiated THP-1 cells were infected at an MOI = 10 for 60 min. followed by lysis
180 with 30ug/mL digitonin in acetate buffer (50 mM Na-acetate pH 5.6, 150 mM NaCl, 0.5 mM EDTA)
181 and protease inhibitors (1X HALT phosphatase/protease inhibitor cocktail (Thermo Fisher
182 Scientific), 100 µM PMSF, 1 µg/mL pepstatin)) (29). The cell lysate was separated into cytosolic and
183 membrane fractions as described above. Cathepsin B activity in cytosolic fractions was measured
184 using the SensoLyte 520 Cathepsin B Assay Kit (AnaSpec) according to the manufacturer's
185 instructions. Relative fluorescence units were normalized to the corresponding protein concentration
186 for each sample and compared with the uninfected cells. Data from 3 independent experiments were
187 combined.

188 **2.10 v-ATPase activity assay**

189 Cell membrane fractions containing lysosomes were prepared using 30ug/mL digitonin in acetate
190 buffer as described above. 10ug of each sample was equilibrated in 200ul assay buffer (10mM
191 HEPES, 5mM MgCl2, 125mM KCl, pH = 7.0) (30) at room temperature for 30 min. in the presence
192 or absence of 200nM bafilomycin (MilliporeSigma). 1mM fresh ATP in 200mM Tris pH = 7 was
193 added to each sample and incubated at room temperature for 2.5 hours. 25ul of the reaction was
194 collected and diluted in ultrapure water, and liberation of free phosphate was measured using the
195 Malachite Green Phosphate Assay Kit according to the manufacturer's instructions (MilliporeSigma).
196 Corrected absorbance values (= A_{sample} - $A_{substrate\ blank}$ - $A_{buffer\ blank}$) were compared with a phosphate
197 standard curve to determine phosphate concentration. v-ATPase activity was calculated as the
198 difference in phosphate concentration between samples incubated with and without bafilomycin.

199 **2.11 Statistical analysis**

200 Growth curve data was analyzed using the Growthcurver package in R (31) and comparison of the
201 intrinsic growth rate (r) and carrying capacity (K) was analyzed by one-way ANOVA and Tukey's
202 post-hoc test. All other data were analyzed using Prism v. 9.3.1 (GraphPad Software), on arcsin
203 transformed data where indicated, by one-way ANOVA with Tukey's (normally distributed data) or
204 Dunnett's or Kruskal-Wallis (nonparametric data) multiple comparison tests. Data in Figures 2D, 2G
205 and Supp. Figure 4B were also analyzed by 2-way ANOVA to ensure day to day experimentation
206 and/or individual counters did not contribute to the differences observed in the data (data not shown).
207 Outliers were assessed by the ROUT method (Q = 1%). For all data presented, ****P<0.0001,
208 ***P<0.001, *P<0.05, n.s., not significant.

209 **3 Results**

210 **3.1 Bacterial trafficking in THP-1 macrophages**

211 Because there are reports that GAS can prevent (14) or allow (16) lysosomal fusion upon
212 phagocytosis, we first examined the intracellular trafficking of GAS in THP-1 macrophages.
213 Bacterial contact with cells was initiated by centrifugation to synchronize macrophage uptake of
214 bacteria and phagolysosomal maturation was monitored by immunofluorescence in a short time
215 course infection experiment (Fig. 1, 2). In agreement with the literature (14,16,32), bacteria were
216 rapidly engulfed by THP-1 cells by our earliest measured time point at 7.5 minutes (Fig. 1B, 2D) and
217 colocalized with the early phagosomal marker EEA-1 (Fig. 2C, D). Interestingly, bacteria in
218 phagosomes also began colocalizing with the lysosomal marker LAMP-1 as early as 7.5 minutes
219 (Fig. 1B). Maximal colocalization with LAMP-1 began at 30 minutes and GAS remained within
220 phagolysosomes throughout the later time points (Fig. 1A, B). Surprisingly, but in agreement with
221 other reports (32), the number of bacteria per cell was relatively constant throughout the experiment
222 (Fig. 1C). These data indicated that bacteria were trafficked as expected to phagolysosomes, but
223 bacteria were held in these compartments without observable bacterial elimination or replication
224 within this time frame. Although we synchronized the infection, there was a possibility that this
225 result was due to continuous infection of macrophages and turnover of bacteria. To address this, we
226 performed the trafficking experiment with a second round of bacterial infection (Fig. 1D). Bacteria
227 introduced in the secondary infection were rarely found in macrophages and were mostly
228 extracellular (Fig. 1D), in agreement with a report for *Salmonella* Typhimurium that the frequency of
229 macrophage reinfection after the primary infection is rare (33). Thus, bacteria from the primary
230 infection persist in THP-1 macrophage phagolysosomes.

231 **3.2 GAS reside in non-acidified phagolysosomes in THP-1 macrophages**

232 Acidification is critical for optimal activity of the proteolytic enzymes in the lysosome (34).
233 Because bacteria appeared to be held in phagolysosomes without observable elimination, we
234 wondered whether phagolysosomes containing GAS were acidified. Lysotracker is an acidotropic
235 dye commonly used to track acidic compartments such as lysosomes in the cell. However, because
236 GAS is an acid-producing bacterial species, we tested whether Lysotracker would be an accurate
237 indicator of lysosomal pH in GAS-infected cells. Although Lysotracker colocalized with lysosomal
238 markers in THP-1 cells, the staining and uptake was inconsistent (Supp. Fig. 1A). Furthermore,
239 bacteria were brightly stained with Lysotracker in both infected cells and in the absence of cells
240 (Supp. Fig. 1A-C). This made it difficult to determine whether and to what extent phagolysosomes
241 containing GAS were acidified. We therefore expressed a pH-sensitive green fluorescent protein
242 variant mWASABI (7) in GAS to monitor phagolysosomal pH of GAS-infected cells (Fig. 2A).
243 Green fluorescence produced by live bacteria was appropriately quenched in low pH environments
244 (Fig. 2A, B). Notably, pH was distinguishable by fluorescence intensity between pH 5.0 and 4.5 (Fig.
245 2B).

246 We infected THP-1 macrophages with mWASABI-expressing GAS and performed a detailed
247 trafficking assay of GAS through the phagolysosomal pathway (Fig. 2C, D). For this experiment, we
248 used the lysosomal protein LAMP-2 to confirm the lysosomal fusion we observed earlier (Fig. 1)
249 since there is conflicting evidence in the literature that GAS prevents lysosomal fusion (13). Because
250 bacteria were tracked by mWASABI expression instead of immunofluorescent staining
251 colocalization with phagosomal markers was difficult (Fig. 2C, D). To quantitate the data, we
252 manually counted bacteria that colocalized with phagolysosomal markers in a blinded manner (Fig.
253 2D). We again found that GAS was initially located in phagosomes, as indicated by EEA-1 staining,
254 which was followed by rapid bacterial colocalization with the mature lysosomal marker LAMP-2
255 within the first 15 minutes of infection (Fig. 2C, D), similar to the colocalization dynamics observed
256 with LAMP-1 staining (Fig. 1). An average of 50% of the counted intracellular bacteria were

257 colocalized with LAMP-2 at the 60 and 90 minute post-infection time points, which was significantly
258 increased compared with the 7.5 minute time point (Fig. 2C, D). Although there were some
259 fluctuations in the number of bacteria in phagolysosomes (Fig. 2E), the number of intracellular
260 bacteria remained relatively constant at all time points, consistent with our initial data (Fig. 1C).
261 Supporting this data, the percentage of infected cells was similar across all time points (Supp. Fig. 2).
262 This corroborated our finding that little to no bacterial eradication or replication was occurring within
263 this time frame (Fig. 2E).

264 Surprisingly, we also found that the green fluorescence signal did not diminish over time,
265 indicating that the intracellular bacteria were not in an acidic environment (Fig. 2C, F). Fluorescence
266 signal intensity of intracellular bacteria in phagolysosomes was not significantly different than that of
267 the extracellular bacteria in our images (Fig. 2F). As the lysosomal lumen is typically between pH
268 4.5–5 when acidified (35), a pH level that our mWASABI probe can differentiate (Fig. 2A, B), these
269 data indicated that GAS were maintained in phagolysosomes that are not appropriately acidified.

270 We confirmed that GAS-infected phagosomes were not acidified with a second method using
271 pH-sensitive FITC-conjugated 70kD dextran particles. Acidification of the lysosomes resulted in
272 quenching of the fluorescence signal in uninfected and control cells infected with immunoglobulin-
273 conjugated beads (Fig. 2G). However, the fluorescence signal was increased in cells infected with all
274 tested strains of GAS, indicating no pH change (Fig. 2G). The low magnitude of difference we
275 observed in our GAS-infected cells compared with the uninfected cells may be due to the limited
276 ability of cells to uptake such a large molecule (70kD) which produced variation between
277 experiments (Fig. 2G). Nevertheless, these results confirmed that GAS-infected phagolysosomes are
278 not properly acidified. Additionally, there are differences in signal between GAS strains (Fig. 2G),
279 but all cells infected with GAS show increased fluorescence signal compared with the uninfected
280 cells. This ability of GAS to prevent lysosomal acidification may account for the persistence of the
281 bacteria in THP-1 cells (Fig. 1C, 2E).

282 **3.3 GAS does not tolerate acidic lysosomal conditions**

283 GAS is a lactic acid-producing bacterial species and possesses systems such as the arginine
284 deiminase (ADI) pathway that confer acid tolerance (36,37). As expected, we found that the final pH
285 of both buffered and unbuffered culture medium after bacterial growth was acidic (Table 1).
286 However, in a physically constrained environment such as the lysosome, the effectiveness of such
287 systems may be limited. The pH of the lysosomal lumen has been reported to range between pH 4.5-
288 5 (35). We wondered whether a pH similar to that found in the lysosome adversely affected bacterial
289 growth and survival. In timed growth experiments, bacteria grown in buffered media adjusted to pH
290 7 had no significant difference in maximum population size, but a statistically significant increase in
291 the intrinsic growth rate of the population compared with unbuffered media (Fig. 3A). Bacteria
292 grown in media adjusted to pH 6 grew at a significantly slower rate and did not reach a similar
293 maximum population size in the time frame of our experiment compared with unbuffered media (Fig.
294 3A). Bacteria grown in media adjusted to pH 5 or lower did not demonstrate measurable growth (Fig.
295 3A). Thus, GAS growth is sensitive to decreasing pH and is inhibited at a pH found in the lysosomal
296 environment.
297
298 The final pH of the stationary phase cultures in both buffered and unbuffered culture media
299 (Table 1) indicated that although GAS may not replicate in acidic conditions, it may be capable of
300 survival. Quantitative plating of cultures at various time points throughout the growth experiment
301 indicated that bacteria in pH 5 media were present (data not shown), but not measurably growing

302 (Fig. 3A). We therefore performed a detailed time course to monitor bacterial survival in low pH
303 media (Fig. 3B). Bacteria incubated in unbuffered media did not significantly grow during the time
304 frame of the survival experiment (data not shown). Similar to other studies (38,39), we found that
305 GAS does not survive in low pH media (Fig. 3B). Although bacteria incubated in up to pH 5.3 media
306 could survive for a short time, bacterial numbers declined at later time points (Fig. 3B), in agreement
307 with pH 5 being the limit at which bacteria can survive (37,40) and the final pH of stationary phase
308 bacterial cultures (Table 1). Our data affirm that GAS cannot survive in the acidified lysosome and
309 therefore, limiting or preventing acidification (Fig. 2) is a survival strategy that GAS may use to
310 persist in phagolysosomes.
311

312 **3.4 Streptolysin O creates large perforations in the phagolysosome**

313 Although GAS has several acid stress response strategies (41), a better tactic may be to avoid
314 the acidification of the phagolysosome altogether. The inability of bacteria to survive in low pH
315 environments (Fig. 3) led us to examine whether GAS infection has a mechanism to prevent
316 phagolysosomal acidification. Pore-forming toxins such as SLO create pores as large as 25-30nm in
317 diameter (17). Others have shown that pore-forming toxins, including SLO, allow escape of
318 hydrogen ions that prevent acidification of the lysosome (16,42). Streptolysin S (SLS) can similarly
319 perforate membranes (43). We fed THP-1 macrophages fluorescent-conjugated molecules and
320 dextrans of various sizes to assess pore size and leakage from phagolysosomes in GAS-infected cells.
321 The ability to measure phagosomal leakage was confirmed using the lysosomal permeabilization
322 agent LLOMe (Supp. Fig. 3). LLOMe permeabilizes lysosomes to molecules up to at least 4.4kD, but
323 not to molecules greater than 10kD (29). Retention of the 10kD, but not the 570Da probe in LLOMe-
324 treated cells confirmed uptake of the probe in phagolysosomes and appropriate release into the
325 cytosol upon permeabilization (Supp. Fig. 3A). Cells loaded with probes of varying sizes were
326 infected with GAS (Fig. 4A, B). As expected, WT GAS caused probes up to 40kD in size,
327 approximately 9nm in diameter (44), to leak from phagolysosomes (Fig. 4A, B). We next used heat-
328 killed bacteria (HK) that retain surface structure but are unable to secrete proteins such as SLO and
329 SLS. We found that the fluorescent probes were retained and colocalized with heat-killed bacteria
330 (Fig. 4A, B), suggesting that a secreted toxin is responsible for leakage. To determine which toxins
331 were responsible for this leakage, we infected cells with bacteria lacking different proteins. ΔSLO
332 GAS-infected cells retained the probes, while cells infected with ΔSagA GAS (lacking SLS) allowed
333 leakage of the probes, similar to the WT strain (Fig. 4A, B). In our assays, SLS did not significantly
334 damage the phagolysosomal membrane, as indicated by the lack of leakage of even the small 570Da
335 probe (Supp. Fig. 3B). Mutant bacteria lacking the surface protein M1 (ΔM1), but with unaltered
336 expression of SLO and SLS behaved similarly to WT strains (Fig. 4A, B). Our data further indicate
337 that SLO allowed probes up to 70kD in size, approximately 13nm in diameter (44), to escape from
338 the lysosomes (Fig. 4B), in agreement with the reported pore size for SLO (17). These data indicate
339 that SLO is the primary pore-forming toxin that perforates the phagolysosome and allows leakage of
340 not only protons, but relatively large proteins.
341

342 Because such large molecules can leak from GAS-infected phagosomes, we next tested
343 whether lysosomal enzymes could escape into the cytosol through SLO-mediated pores. We infected
344 cells with WT or ΔSLO GAS and collected membrane and cytosolic cell fractions. Lack of lysosomal
345 markers in the cytosolic fraction indicated little to no contamination of the cytosolic fraction with
346 lysosomes (Fig. 4C). The membrane fraction contained most of the lysosomal enzyme cathepsin B as
347 expected (Fig. 4C). However, we noted a small, but visible increase in the amount of cathepsin B
348 present in the cytosolic fraction of WT-infected cells compared with uninfected and ΔSLO-infected

349 cells (Fig. 4C). In order to verify that cathepsin B was present in the cytosol, we measured cathepsin
350 B activity in the cytosolic fraction. Cytosolic fractions from WT-infected cells contained the highest
351 amount of cathepsin B activity compared with uninfected cells (Fig. 4D). Cytosolic fractions from
352 ΔSLO-infected cells (Fig. 4B) did not exhibit cathepsin B activity higher than uninfected cells (Fig.
353 4D). These data confirmed that SLO secreted by WT bacteria perforates the phagolysosomal
354 membrane and allows the leakage of large proteins such as the lysosomal enzyme cathepsin B into
355 the cytosol. This loss of proteolytic enzymes from the phagolysosome in addition to the loss of
356 protons likely contributes to the ability of GAS to persist in the phagolysosome during infection.

357 **3.5 GAS prevents proper function of vacuolar ATPase**

358 Although SLO-mediated pores could cause leakage of protons from the phagolysosome,
359 reports in the literature also suggest that the v-ATPase that is required for acidification of the
360 lysosome is non-functional in GAS-infected cells (20). Supporting this, we found that the
361 phagolysosomes of macrophages infected with ΔSLO and heat-killed bacteria were also not acidified
362 (Fig. 2G). Furthermore, ΔSLO bacteria are trafficked to phagolysosomes, maintain the fluorescent
363 signal of mWASABI, and are maintained at constant numbers in THP-1 cells similar to WT bacteria
364 (Supp. Fig. 4). These data are consistent with the idea that phagolysosomes infected with ΔSLO
365 bacteria are also not acidified. We therefore investigated whether v-ATPase is properly assembled
366 and functional in GAS-infected cells. v-ATPase consists of the membrane-bound F_0 subunit
367 (containing the V_0D_1 protein) that must assemble with the cytosolic F_1 subunit (containing the V_1A
368 protein) for proper function (28). We monitored v-ATPase assembly by tracking movement of the
369 V_1A subunit from the cytosolic to membrane fractions. Cells fed Ig-conjugated beads (Ab beads)
370 were included as a positive control (Fig. 5A, B). We observed no difference in v-ATPase subunit
371 assembly in cells infected with GAS compared to Ab bead-fed or uninfected cells (Fig. 5A, B),
372 indicating that the acidification machinery was recruited properly to phagolysosomes. However,
373 when we measured v-ATPase activity in membrane fractions of GAS-infected cells, we found
374 significantly decreased v-ATPase activity in fractions from cells infected with all strains of GAS
375 compared with uninfected cells (Fig. 5C). These data are in agreement with the lack of acidification
376 in GAS-infected cells observed in our experiments using pH-sensitive dextrans (Fig. 2G). Therefore,
377 though the v-ATPase is properly assembled in GAS-infected cells, the activity of this enzyme is
378 limited, preventing proper acidification of the phagolysosome. Thus, our data suggests that GAS
379 persists in macrophages by employing a multi-pronged approach to avoid the acidification and
380 destructive mechanisms of the phagolysosome.

381 **4 Discussion**

382 The human-specific pathogen GAS has co-evolved with the human immune system, and has
383 multiple mechanisms for survival within the host (1,12). Although GAS is an extracellular bacterial
384 pathogen, phagocytic cells such as macrophages can readily engulf bacteria (14,16,32). The ability of
385 GAS to not only survive in macrophages, but to potentially alter their function, escape downstream
386 immune responses, and be sheltered from antibiotic treatment provides a basis for successful
387 persistence in humans.

388 In our experiments, we found that GAS was readily phagocytosed and phagosomes quickly
389 fused with lysosomes, but that GAS remained in these compartments (Fig. 1, 2). There is conflicting
390 evidence in the literature about whether lysosomes fuse with GAS-containing phagosomes in
391 macrophages, which may be due to a difference in cell origin or source of antibodies (14,16). We
392 find that in THP-1 macrophages, lysosomal fusion with GAS-containing phagosomes occurs, as

393 confirmed by colocalization with two independent lysosomal antibodies (Fig. 1, 2). We recognize
394 that although our studies may be limited due to the exclusive use of cell culture, our data are in
395 agreement with several studies regarding lysosomal fusion with GAS-infected phagosomes (16,32).
396 In addition, we corroborated previous data that SLO induces perforation and damage of the
397 phagolysosomal membrane (Fig. 4) (16,45) which promotes bacterial survival. In addition to loss of
398 lysosomal enzymes and protons, we also demonstrated that GAS limits phagolysosomal acidification
399 to increase bacterial survival (Fig. 2, 5). Although ΔSLO GAS also prevented phagolysosomal
400 acidification (Fig. 2, 5), others have shown that ΔSLO GAS are less fit for survival in macrophages
401 and other cells (16,46). ΔSLO GAS is likely still susceptible to other macrophage killing mechanisms
402 such as reactive oxygen species or xenophagy (46). Finally, our data demonstrate that bacteria persist
403 in phagolysosomes without replication or escape into the cytosol (Fig. 1, 2, Supp. Fig. 4) (14,16).
404 This is in agreement with another study of GAS in THP-1 cells (32), but different from what has
405 previously been observed in epithelial and U-937 cells, where GAS escapes into the cytosol and
406 replicates (15,32,45). In our experiments, not all GAS were in LAMP-positive compartments (Fig. 1,
407 2), which may be due to lysophagic clearance of GAS-damaged lysosomal membranes (32,47).
408 However, the downstream fate of GAS in non-functional lysosomes in THP-1 macrophages remains
409 to be elucidated.

410 The pH of the lysosomal lumen has been reported to range between pH 4.5-5 (35). However,
411 we found that acidified medium was sufficient to kill GAS (Fig. 3). These results are somewhat
412 surprising since not only does GAS produce lactic acid, but previous reports suggest GAS has
413 multiple mechanisms for acid tolerance, including a F_0/F_1 proton pump and the arginine deiminase
414 pathway which produces alkali (36,37,41,48). However, there may be a limit to which these systems
415 work, especially within an enclosed environment such as in vitro conditions or in the phagolysosome,
416 as demonstrated by the threshold for bacterial survival in low pH medium (Fig. 3) (37). Additionally,
417 GAS lacks enzymes such as glutamate decarboxylase and urease (41), making neutralization of
418 highly acidified environments a less viable strategy. Therefore, two mechanisms to prevent
419 acidification, perforating the phagolysosomal membrane (Fig. 4) and blocking v-ATPase activity
420 (Fig. 5) provide a means to survive within the phagolysosomal compartment. Other bacteria such as
421 *Legionella pneumophila* have proteins such as SidK, which binds v-ATPase subunits to prevent
422 activity (30). Our data indicate that neither SLO nor any other secreted factor is responsible for
423 interfering with v-ATPase activity (Fig. 5C), and the identity of the GAS protein(s) responsible for
424 inhibiting v-ATPase activity remains to be elucidated.

425 Previous data and our results indicate SLO causes leakage of lysosomal contents (Fig. 4).
426 These proteins include active lysosomal enzymes such as cathepsin B (Fig. 4). The cathepsin B
427 activity we measured was subtle, likely because the enzyme optimally functions in a low pH
428 environment (8), which is neither achieved in GAS-infected lysosomes (Fig. 2, 5) nor in the cytosol.
429 However, releasing active lysosomal proteases could have downstream effects on the cell such as
430 activation of the NLRP3 inflammasome and pyroptosis (49). Furthermore, SLO promotes
431 macrophage apoptosis by releasing SLO from the lysosome and causing mitochondrial damage
432 (22,50). Other proteins released from the infected lysosome could also include bacterial proteases
433 such as SpeB, whose presence in the cytosol could lead to NLRP3 inflammasome activation and
434 release of the proinflammatory cytokine IL-1β (51–55). Persistent IL-1β activation as a result of GAS
435 infection has been linked with ARF and rheumatic heart disease (56). Thus, besides enabling
436 bacterial survival and blunting the normal macrophage response, this alternative macrophage
437 response may lead to pathologies such as ARF that are observed during GAS infection. Studies have
438 shown that macrophages are crucial for GAS clearance (2), but the loss of macrophage function may
439 also have detrimental effects on the long-term response to GAS infection, including the inability to

generate protective antibodies. Therapies aimed at improving macrophage function may therefore improve GAS infection outcomes. Although SLO is a promising target, our work shows that additional drugs to restore v-ATPase activity would be necessary to fully restore macrophage function. Restoration of macrophage function in GAS infection would allow individuals to mount a proper adaptive immune response to confer protective immunity.

5 Conflict of Interest

The authors declare that the research was conducted in the absence of any commercial or financial relationships that could be construed as a potential conflict of interest.

6 Author Contributions

SN, JS, AT and CO contributed to conception and design of the study. All authors performed the experiments and analyzed data. CO wrote the first draft of the manuscript. All authors contributed to manuscript revision, read, and approved the submitted version.

7 Funding

Support for this project has been provided by the American Heart Association (17GRNT33410851 to CO), the Fletcher Jones Science Scholars Fellowship (to SN), the Occidental College Undergraduate Research Center (to SN, JS, JL, JS, RZ and HA), the Kurata Faculty Excellence Award (to CO), Occidental College (to CO) and the San Diego Center for Systems Biology (to AT).

8 Acknowledgments

We thank Cheldon Alcantara and Ryan Hino for contributions to experiments, Karen Molinder for helpful discussions and Kelvin Zheng, Jessica Kim, Stephanie Peacock, Isabel Perez, Kevin Kim, and the Fall 2021 Bio 395 GRR course for contributions to data analysis in this paper.

9 References

1. Sims Sanyahumbi A, Colquhoun S, Wyber R, Carapetis JR. Global Disease Burden of Group A Streptococcus. In: Ferretti JJ, Stevens DL, Fischetti VA, editors. Streptococcus pyogenes : Basic Biology to Clinical Manifestations [Internet]. Oklahoma City (OK): University of Oklahoma Health Sciences Center; 2016 [cited 2022 Apr 11]. Available from: http://www.ncbi.nlm.nih.gov/books/NBK333415/

2. Goldmann O, Rohde M, Chhatwal GS, Medina E. Role of Macrophages in Host Resistance to Group A Streptococci. Infect Immun. 2004 May;72(5):2956–63.

3. Mishalian I, Ordan M, Peled A, Maly A, Eichenbaum MB, Ravins M, et al. Recruited macrophages control dissemination of group A Streptococcus from infected soft tissues. J Immunol Baltim Md 1950. 2011 Dec 1;187(11):6022–31.

4. Thulin P, Johansson L, Low DE, Gan BS, Kotb M, McGeer A, et al. Viable group A streptococci in macrophages during acute soft tissue infection. PLoS Med. 2006 Mar;3(3):e53.

474 5. Österlund A, Popa R, Nikkilä T, Scheynius A, Engstrand L. Intracellular Reservoir of
475 Streptococcus pyogenes In Vivo: A Possible Explanation for Recurrent Pharyngotonsillitis. The
476 Laryngoscope. 1997;107(5):640–7.

477 6. Johnson AF, LaRock CN. Antibiotic Treatment, Mechanisms for Failure, and Adjunctive
478 Therapies for Infections by Group A Streptococcus. Front Microbiol. 2021;12:760255.

479 7. Zhou C, Zhong W, Zhou J, Sheng F, Fang Z, Wei Y, et al. Monitoring autophagic flux by an
480 improved tandem fluorescent-tagged LC3 (mTagRFP-mWasabi-LC3) reveals that high-dose
481 rapamycin impairs autophagic flux in cancer cells. Autophagy. 2012 Aug;8(8):1215–26.

482 8. Flannagan RS, Heit B, Heinrichs DE. Antimicrobial Mechanisms of Macrophages and the
483 Immune Evasion Strategies of Staphylococcus aureus. Pathogens. 2015 Dec;4(4):826–68.

484 9. Carranza C, Chavez-Galan L. Several Routes to the Same Destination: Inhibition of
485 Phagosome-Lysosome Fusion by Mycobacterium tuberculosis. Am J Med Sci. 2019
486 Mar;357(3):184–94.

487 10. Misch EA. Legionella: virulence factors and host response. Curr Opin Infect Dis. 2016
488 Jun;29(3):280–6.

489 11. Ganem MB, De Marzi MC, Fernández-Lynch MJ, Jancic C, Vermeulen M, Geffner J, et al.
490 Uptake and intracellular trafficking of superantigens in dendritic cells. PloS One.
491 2013;8(6):e66244.

492 12. Siemens N, Snäll J, Svensson M, Norrby-Teglund A. Pathogenic Mechanisms of Streptococcal
493 Necrotizing Soft Tissue Infections. Adv Exp Med Biol. 2020;1294:127–50.

494 13. Staali L, Bauer S, Mörgelin M, Björck L, Tapper H. Streptococcus pyogenes bacteria modulate
495 membrane traffic in human neutrophils and selectively inhibit azurophilic granule fusion with
496 phagosomes. Cell Microbiol. 2006 Apr;8(4):690–703.

497 14. Hertzén E, Johansson L, Wallin R, Schmidt H, Kroll M, Rehn AP, et al. M1 protein-dependent
498 intracellular trafficking promotes persistence and replication of Streptococcus pyogenes in
499 macrophages. J Innate Immun. 2010;2(6):534–45.

500 15. Walker MJ, Barnett TC, McArthur JD, Cole JN, Gillen CM, Henningham A, et al. Disease
501 Manifestations and Pathogenic Mechanisms of Group A Streptococcus. Clin Microbiol Rev.
502 2014 Apr 1;27(2):264–301.

503 16. Bastiat-Sempe B, Love JF, Lomayesva N, Wessels MR. Streptolysin O and NAD-
504 glycohydrolase prevent phagolysosome acidification and promote group A Streptococcus
505 survival in macrophages. mBio. 2014 Sep 16;5(5):e01690-01614.

506 17. Bhakdi S, Tranum-Jensen J, Sziegoleit A. Mechanism of membrane damage by streptolysin-O.
507 Infect Immun. 1985 Jan;47(1):52–60.

508 18. Buckingham L, Duncan JL. Approximate dimensions of membrane lesions produced by
509 streptolysin S and streptolysin O. Biochim Biophys Acta. 1983 Mar 23;729(1):115–22.

510 19. Håkansson A, Bentley CC, Shakhnovic EA, Wessels MR. Cytolysin-dependent evasion of
511 lysosomal killing. Proc Natl Acad Sci U S A. 2005 Apr 5;102(14):5192–7.

512 20. Nordenfelt P, Grinstein S, Björck L, Tapper H. V-ATPase-mediated phagosomal acidification is
513 impaired by Streptococcus pyogenes through Mga-regulated surface proteins. Microbes Infect.
514 2012 Nov;14(14):1319–29.

515 21. Chatellier S, Ihendyane N, Kansal RG, Khambaty F, Basma H, Norrby-Teglund A, et al.
516 Genetic relatedness and superantigen expression in group A streptococcus serotype M1 isolates
517 from patients with severe and nonsevere invasive diseases. Infect Immun. 2000 Jun;68(6):3523–
518 34.

519 22. Timmer AM, Timmer JC, Pence MA, Hsu LC, Ghochani M, Frey TG, et al. Streptolysin O
520 promotes group A Streptococcus immune evasion by accelerated macrophage apoptosis. J Biol
521 Chem. 2009 Jan 9;284(2):862–71.

522 23. Lauth X, von Köckritz-Blickwede M, McNamara CW, Myskowski S, Zinkernagel AS, Beall B,
523 et al. M1 protein allows Group A streptococcal survival in phagocyte extracellular traps through
524 cathelicidin inhibition. J Innate Immun. 2009;1(3):202–14.

525 24. Datta V, Myskowski SM, Kwinn LA, Chiem DN, Varki N, Kansal RG, et al. Mutational
526 analysis of the group A streptococcal operon encoding streptolysin S and its virulence role in
527 invasive infection. Mol Microbiol. 2005 May;56(3):681–95.

528 25. Ai H wang, Olenych SG, Wong P, Davidson MW, Campbell RE. Hue-shifted monomeric
529 variants of Clavularia cyan fluorescent protein: identification of the molecular determinants of
530 color and applications in fluorescence imaging. BMC Biol. 2008 Mar 6;6:13.

531 26. Jeng A, Sakota V, Li Z, Datta V, Beall B, Nizet V. Molecular genetic analysis of a group A
532 Streptococcus operon encoding serum opacity factor and a novel fibronectin-binding protein,
533 SfbX. J Bacteriol. 2003 Feb;185(4):1208–17.

534 27. McQuin C, Goodman A, Chernyshev V, Kamentsky L, Cimini BA, Karhohs KW, et al.
535 CellProfiler 3.0: Next-generation image processing for biology. PLoS Biol. 2018
536 Jul;16(7):e2005970.

537 28. McGuire CM, Forgac M. Glucose starvation increases V-ATPase assembly and activity in
538 mammalian cells through AMP kinase and phosphatidylinositide 3-kinase/Akt signaling. J Biol
539 Chem. 2018 Jun 8;293(23):9113–23.

540 29. Repnik U, Borg Distefano M, Speth MT, Ng MYW, Progida C, Hoflack B, et al. L-leucyl-L-
541 leucine methyl ester does not release cysteine cathepsins to the cytosol but inactivates them in
542 transiently permeabilized lysosomes. J Cell Sci. 2017 Sep 15;130(18):3124–40.

543 30. Xu L, Shen X, Bryan A, Banga S, Swanson MS, Luo ZQ. Inhibition of host vacuolar H+-
544 ATPase activity by a Legionella pneumophila effector. PLoS Pathog. 2010 Mar
545 19;6(3):e1000822.

546 31. Sprouffske K, Wagner A. Growthcurver: an R package for obtaining interpretable metrics from
547 microbial growth curves. BMC Bioinformatics. 2016 Apr 19;17:172.

548 32. O'Neill AM, Thurston TLM, Holden DW. Cytosolic Replication of Group A Streptococcus in
549 Human Macrophages. mBio. 2016 Apr 12;7(2):e00020-00016.

550 33. Gog JR, Murcia A, Osterman N, Restif O, McKinley TJ, Sheppard M, et al. Dynamics of
551 Salmonella infection of macrophages at the single cell level. J R Soc Interface. 2012 May
552 2;9(75):2696–707.

553 34. Bright NA, Davis LJ, Luzio JP. Endolysosomes Are the Principal Intracellular Sites of Acid
554 Hydrolase Activity. Curr Biol CB. 2016 Sep 12;26(17):2233–45.

555 35. Canton J, Grinstein S. Chapter 5 - Measuring lysosomal pH by fluorescence microscopy. In:
556 Platt F, Platt N, editors. Methods in Cell Biology [Internet]. Academic Press; 2015 [cited 2021
557 Jul 1]. p. 85–99. (Lysosomes and Lysosomal Diseases; vol. 126). Available from:
558 https://www.sciencedirect.com/science/article/pii/S0091679X14000223

559 36. Degnan BA, Fontaine MC, Doebereiner AH, Lee JJ, Mastroeni P, Dougan G, et al.
560 Characterization of an isogenic mutant of Streptococcus pyogenes Manfredo lacking the ability
561 to make streptococcal acid glycoprotein. Infect Immun. 2000 May;68(5):2441–8.

562 37. Cusumano ZT, Caparon MG. Citrulline protects Streptococcus pyogenes from acid stress using
563 the arginine deiminase pathway and the F1Fo-ATPase. J Bacteriol. 2015 Apr;197(7):1288–96.

564 38. Maudsdotter L, Jonsson H, Roos S, Jonsson AB. Lactobacilli reduce cell cytotoxicity caused by
565 Streptococcus pyogenes by producing lactic acid that degrades the toxic component lipoteichoic
566 acid. Antimicrob Agents Chemother. 2011 Apr;55(4):1622–8.

567 39. Daglia M, Papetti A, Grisoli P, Aceti C, Dacarro C, Gazzani G. Antibacterial activity of red and
568 white wine against oral streptococci. J Agric Food Chem. 2007 Jun 27;55(13):5038–42.

569 40. Jin H, Agarwal S, Agarwal S, Pancholi V. Surface export of GAPDH/SDH, a glycolytic
570 enzyme, is essential for Streptococcus pyogenes virulence. mBio. 2011;2(3):e00068-00011.

571 41. Cotter PD, Hill C. Surviving the acid test: responses of gram-positive bacteria to low pH.
572 Microbiol Mol Biol Rev MMBR. 2003 Sep;67(3):429–53.

573 42. Shaughnessy LM, Hoppe AD, Christensen KA, Swanson JA. Membrane perforations inhibit
574 lysosome fusion by altering pH and calcium in Listeria monocytogenes vacuoles. Cell
575 Microbiol. 2006 May;8(5):781–92.

576 43. Molloy EM, Cotter PD, Hill C, Mitchell DA, Ross RP. Streptolysin S-like virulence factors: the
577 continuing sagA. Nat Rev Microbiol. 2011 Sep;9(9):670–81.

578 44. Ambati J, Canakis CS, Miller JW, Gragoudas ES, Edwards A, Weissgold DJ, et al. Diffusion of
579 high molecular weight compounds through sclera. Invest Ophthalmol Vis Sci. 2000
580 Apr;41(5):1181–5.

581 45. Cheng YL, Wu YW, Kuo CF, Lu SL, Liu FT, Anderson R, et al. Galectin-3 Inhibits Galectin-
582 8/Parkin-Mediated Ubiquitination of Group A Streptococcus. mBio. 2017 Jul 25;8(4):e00899-
583 17.

584 46. O'Seaghdha M, Wessels MR. Streptolysin O and its co-toxin NAD-glycohydrolase protect
585 group A Streptococcus from Xenophagic killing. PLoS Pathog. 2013;9(6):e1003394.

586 47. Barnett TC, Liebl D, Seymour LM, Gillen CM, Lim JY, Larock CN, et al. The globally
587 disseminated M1T1 clone of group A Streptococcus evades autophagy for intracellular
588 replication. Cell Host Microbe. 2013 Dec 11;14(6):675–82.

589 48. Cusumano ZT, Watson ME, Caparon MG. Streptococcus pyogenes arginine and citrulline
590 catabolism promotes infection and modulates innate immunity. Infect Immun. 2014
591 Jan;82(1):233–42.

592 49. Chevriaux A, Pilot T, Derangère V, Simonin H, Martine P, Chalmin F, et al. Cathepsin B Is
593 Required for NLRP3 Inflammasome Activation in Macrophages, Through NLRP3 Interaction.
594 Front Cell Dev Biol. 2020;8:167.

595 50. Cortés G, Wessels MR. Inhibition of dendritic cell maturation by group A Streptococcus. J
596 Infect Dis. 2009 Oct 1;200(7):1152–61.

597 51. Keyel PA, Roth R, Yokoyama WM, Heuser JE, Salter RD. Reduction of streptolysin O (SLO)
598 pore-forming activity enhances inflammasome activation. Toxins. 2013 Jun 6;5(6):1105–18.

599 52. Chu J, Thomas LM, Watkins SC, Franchi L, Núñez G, Salter RD. Cholesterol-dependent
600 cytolysins induce rapid release of mature IL-1beta from murine macrophages in a NLRP3
601 inflammasome and cathepsin B-dependent manner. J Leukoc Biol. 2009 Nov;86(5):1227–38.

602 53. Richter J, Monteleone MM, Cork AJ, Barnett TC, Nizet V, Brouwer S, et al. Streptolysins are
603 the primary inflammasome activators in macrophages during Streptococcus pyogenes infection.
604 Immunol Cell Biol. 2021 Nov;99(10):1040–52.

605 54. LaRock DL, Russell R, Johnson AF, Wilde S, LaRock CN. Group A Streptococcus Infection of
606 the Nasopharynx Requires Proinflammatory Signaling through the Interleukin-1 Receptor.
607 Infect Immun. 2020 Sep 18;88(10):e00356-20.

608 55. Campden RI, Zhang Y. The role of lysosomal cysteine cathepsins in NLRP3 inflammasome
609 activation. Arch Biochem Biophys. 2019 Jul 30;670:32–42.

610 56. Kim ML, Martin WJ, Minigo G, Keeble JL, Garnham AL, Pacini G, et al. Dysregulated IL-1β-
611 GM-CSF Axis in Acute Rheumatic Fever That Is Limited by Hydroxychloroquine. Circulation.
612 2018 Dec 4;138(23):2648–61.

613

614 **10 Tables**

615 **Table 1: Final pH of media after bacterial growth, mean ± SD**

starting pH	4.0	5.0	6.0	7.0	unbuffered THB (6.6)
ending pH	4.10 ± 0.02	5.07 ± 0.02	4.99 ± 0.01	5.23 ± 0.08	5.63 ± 0.06

616 **11 Figure legends**

617 **Figure 1: GAS persists in phagolysosomes of THP-1 cells. (A,B)** THP-1 cells were infected with
618 GAS for the indicated times, fixed and probed with anti-LAMP-1 and secondary fluorescent
619 antibodies (green). Bacteria opsonized with human serum were detected with anti-human IgG
620 antibody (red). **(A)** Representative image of LAMP-1 colocalized with GAS in THP-1 cells at 60
621 min. post-infection. Arrowheads indicate examples of colocalization. Scale bar = 5µm. **(B)**
622 Quantitation of LAMP-1 positive bacteria at the indicated time points. **(C)** Average number of
623 bacteria per cell at the indicated time points. **(D)** Representative image of THP-1 cells exposed to a
624 primary (green only) GAS infection for 30 min. followed by a secondary (cyan and green) infection
625 for 30 min. (60 min. total infection time). LAMP-1 staining is indicated in red. Arrowheads indicate
626 examples of colocalization between primary infecting GAS and LAMP-1. Arrows indicate GAS from
627 the secondary infection. Scale bar = 5µm. For all graphs, >100 cells were counted, data from three
628 independent experiments were combined and results are given as mean ± 95% CI. Data were
629 analyzed on arcsin transformed data by one-way ANOVA with Tukey's multiple comparisons test.

630 **Figure 2: GAS persists in non-acidified phagolysosomes of THP-1 cells. (A)** GAS expressing
631 mWASABI were incubated in media at the indicated pH for 1 hour. Representative green
632 fluorescence (mWASABI) and brightfield images are shown. Scale bar = 5µm. **(B)** Corrected total
633 cell fluorescence of green fluorescence signal from bacteria expressing mWASABI incubated in
634 media at the indicated pH for 1 hour. **(C)** Representative fluorescence microscopy images of GAS-
635 infected THP-1 cells at 7.5 and 60 min. post-infection. Arrows denote examples of bacteria
636 encapsulated in early phagosomes (EEA-1, magenta), arrowheads denote examples of bacteria
637 encapsulated in phagolysosomes (LAMP-2, red). All images were taken with a 63x objective with 2x
638 digital zoom, scale bar = 5µm. **(D)** Quantitation of bacteria colocalized with phagosomes (EEA-1) or
639 phagolysosomes (LAMP-2) at the indicated time points. **(E)** Average number of bacteria per cell at
640 the indicated time points. **(F)** Violin plot of fluorescence signal intensity from intracellular (clear
641 bars) or extracellular (shaded bars) bacteria expressing mWASABI. **(G)** Fluorescence signal from
642 cells fed 70kD FITC dextran and infected with immunoglobulin-conjugated beads (Ab beads), the
643 indicated GAS strain or heat-killed (HK) bacteria was measured by plate reader. Statistical
644 differences were calculated by comparing samples to uninfected cells. Data from at least three
645 independent experiments were combined. For (D) and (E), >100 cells were counted, data from at
646 least 3 individual counters of at least three independent experiments are shown. Results are given as
647 mean ± 95% CI and statistics were performed on arcsin transformed data by one-way ANOVA with
648 Dunnett's multiple comparisons test.

649 **Figure 3: GAS does not survive in low pH environments. (A)** Growth curves of bacteria grown in
650 buffered media or unbuffered bacterial media (THB) at the indicated pH. Results are given as mean ±
651 95% CI. Statistics in (A) indicate differences in intrinsic growth rate compared with bacteria grown
652 in unbuffered media tested by one-way ANOVA with Tukey's multiple comparisons test. **(B)**
653 Bacterial survival in buffered media at the indicated pH compared with survival of bacteria in
654 unbuffered bacterial media (THB). Statistics in (B) indicate differences in area under the curve
655 compared with bacteria grown in pH = 5.3 media tested by one-way ANOVA with Tukey's multiple
656 comparisons test. For each experiment, samples were prepared in triplicate and data from at least
657 three independent experiments were combined and results are given as mean ± SEM.

658 **Figure 4: SLO induces phagolysosomal perforation and protein leakage. (A)** Representative
659 images of the 40kD dextran probe (top panels, green in merged images) with indicated bacterial
660 strains (middle panels, magenta in merged images). All images were taken with a 63x objective with
661 2x digital zoom, scale bar = 5μm. **(B)** Quantitation of colocalization of indicated bacterial strains
662 with 10, 40 and 70kD dextran probes, >100 cells were counted. **(C)** Cells were infected with the
663 indicated bacterial strains, fractionated into membrane (left) and cytosolic (right) fractions, and
664 probed with the indicated antibodies: LAMP-2 (lysosomal marker; loading control for membrane
665 fraction), GAPDH (cytosolic marker; loading control for cytosolic fraction) and cathepsin B
666 (lysosomal enzyme). **(D)** Cathepsin B activity was measured in cytosolic cell fractions collected from
667 cells infected with the indicated strains. Data were normalized to the corresponding protein
668 concentration for each sample and compared with the uninfected cells. Data in (B) and (D) are
669 combined from at least three independent experiments. Results are given as mean ± 95% CI and and
670 statistics were performed on arcsin transformed data by one-way ANOVA with Tukey's multiple
671 comparison test (B) or one-way ANOVA with Kruskal-Wallis multiple comparison test (D).

672 **Figure 5: GAS infection limits v-ATPase activity. (A)** Cells were uninfected, infected with
673 immunoglobulin-conjugated beads (Ab beads, control), the indicated GAS strain or heat-killed (HK)
674 bacteria and fractionated into membrane (M) and cytosolic (C) fractions. Fractions were probed with
675 antibodies to V_1A, V_0D or GAPDH proteins. Representative data are shown. **(B)** Quantitation of data
676 shown in (A). V_1A band intensities were quantified and normalized to V_0D (membrane) or GAPDH
677 (cytosol). Relative assembly was calculated as the amount of V_1A in the membrane fraction of the
678 indicated infected sample compared with the uninfected sample for each experiment. **(C)** v-ATPase
679 activity assay in membrane fractions from cells infected with the indicated GAS strain. v-ATPase
680 activity was calculated by determining the concentration of free phosphate (released by the ATPase)
681 of the samples and subtracting the concentration of free phosphate in samples incubated with
682 bafilomycin (v-ATPase inhibitor) from the samples incubated without bafilomycin. Data in (B) and
683 (C) are combined from at least three independent experiments and results are given as mean ± 95%
684 CI and analyzed by one-way ANOVA with Tukey's multiple comparison test.

Figure 1

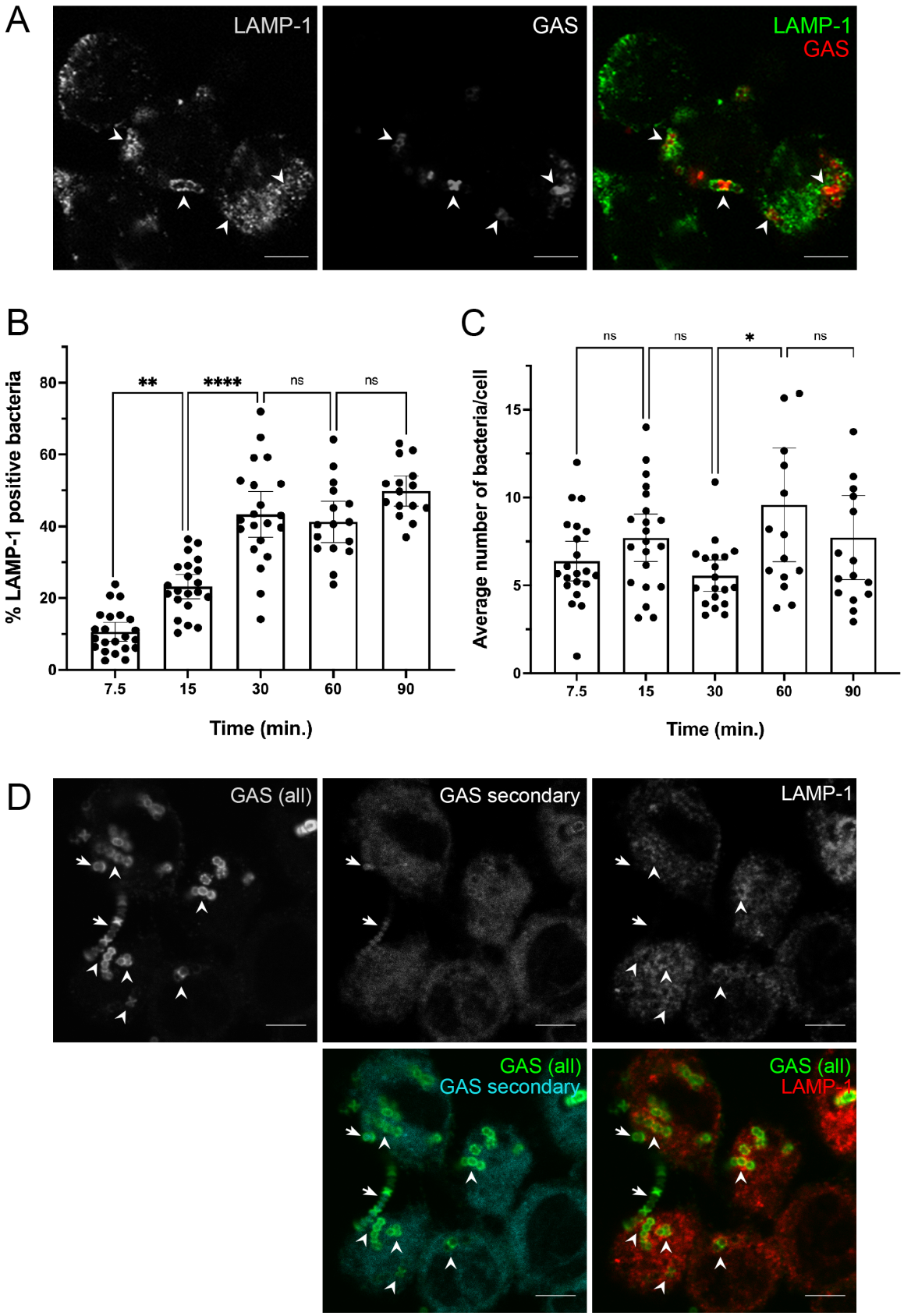
A
LAMP-1
GAS
LAMP-1
GAS
B
% LAMP-1 positive bacteria
0
20
40
60
80
**
****
ns
ns
7.5
15
30
60
90
Time (min.)
C
Average number of bacteria/cell
0
5
10
15
ns
ns
*
ns
7.5
15
30
60
90
Time (min.)
D
GAS (all)
GAS secondary
LAMP-1
GAS (all)
GAS secondary
GAS (all)
LAMP-1

Figure 2

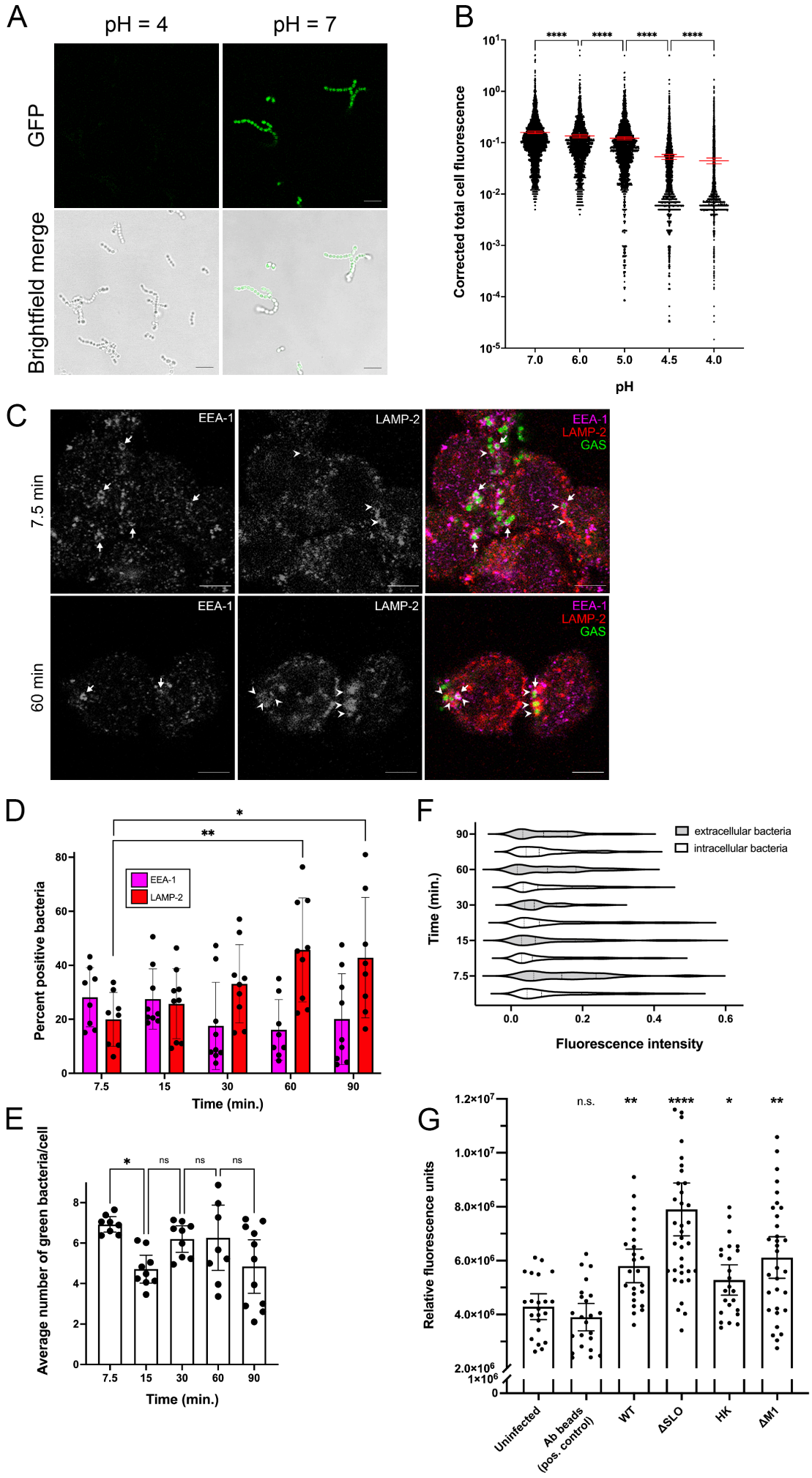
A
pH = 4
pH = 7
GFP
Brightfield merge
B
Corrected total cell fluorescence
pH
7.0
6.0
5.0
4.5
4.0
****
C
7.5 min
60 min
EEA-1
LAMP-2
GAS
D
Percent positive bacteria
Time (min.)
7.5
15
30
60
90
*
**
E
Average number of green bacteria/cell
ns
F
Time (min.)
Fluorescence intensity
extracellular bacteria
intracellular bacteria
G
Relative fluorescence units
n.s.
Uninfected
Ab beads (pos. control)
WT
ΔSLO
HK
ΔM1

Figure 3

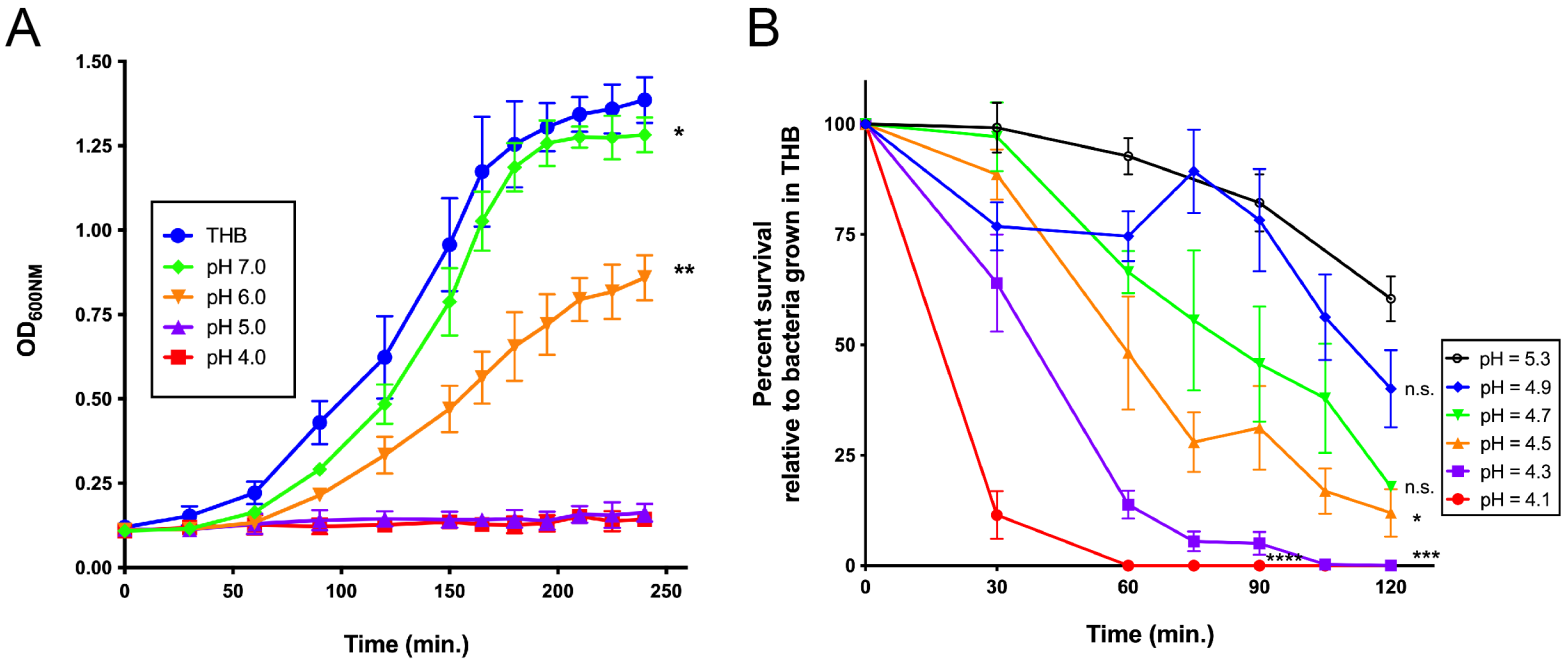
A
1.50
1.25
1.00
0.75
0.50
0.25
0.00
OD600NM
0
50
100
150
200
250
Time (min.)
THB
pH 7.0
pH 6.0
pH 5.0
pH 4.0
*
**
B
100
75
50
25
0
Percent survival
relative to bacteria grown in THB
0
30
60
90
120
Time (min.)
pH = 5.3
pH = 4.9
pH = 4.7
pH = 4.5
pH = 4.3
pH = 4.1
n.s.
n.s.
*
****
***

Figure 4

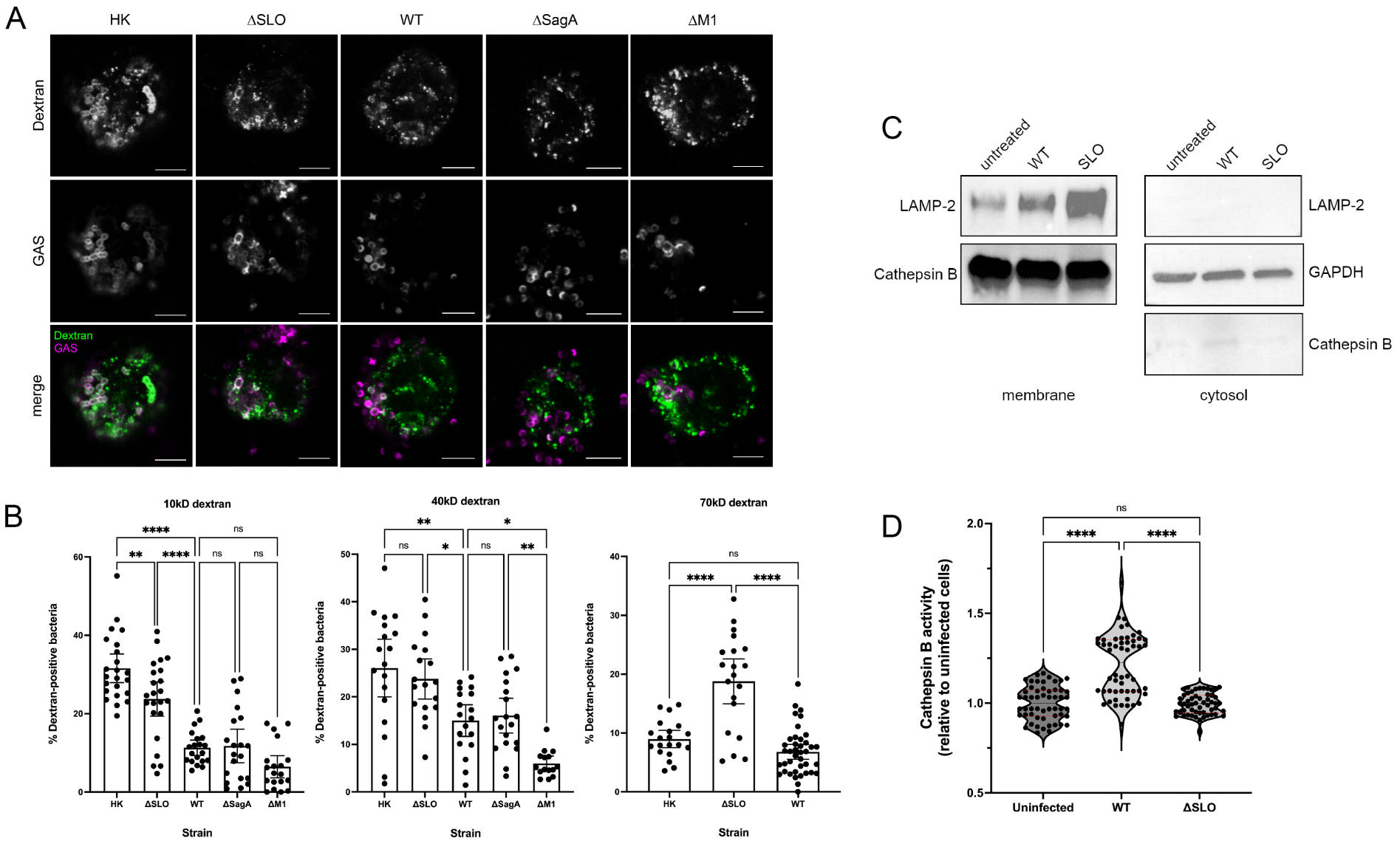
A
HK
ΔSLO
WT
ΔSagA
ΔM1
Dextran
GAS
merge
Dextran
GAS
B
10kD dextran
40kD dextran
70kD dextran
% Dextran-positive bacteria
Strain
HK
ΔSLO
WT
ΔSagA
ΔM1
****
**
ns
*
C
untreated
WT
SLO
LAMP-2
Cathepsin B
GAPDH
membrane
cytosol
D
Cathepsin B activity
(relative to uninfected cells)
Uninfected
WT
ΔSLO
ns
****

Figure 5

A

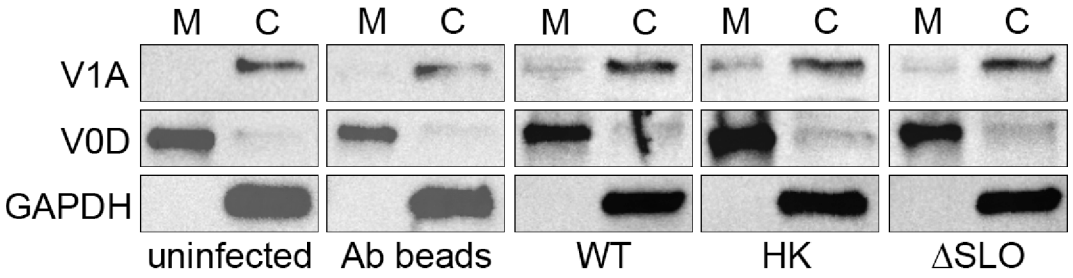
M C M C M C M C M C
V1A
V0D
GAPDH
uninfected
Ab beads
WT
HK
ΔSLO

B

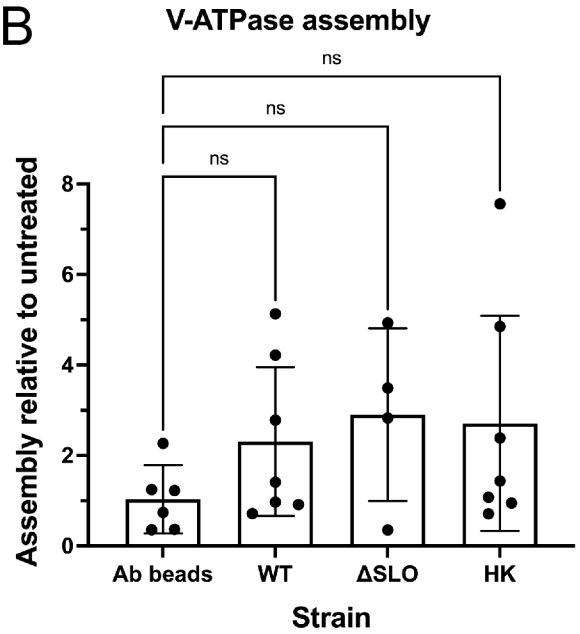
V-ATPase assembly
ns
ns
ns
Assembly relative to untreated
0
2
4
6
8
Ab beads
WT
ΔSLO
HK
Strain

C

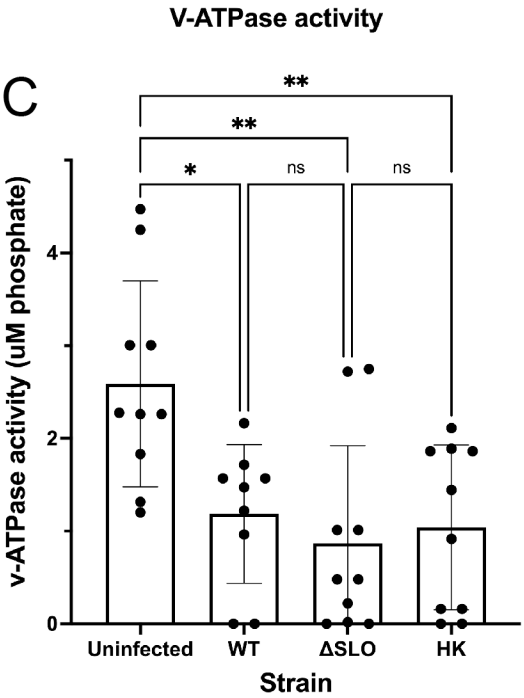
V-ATPase activity
**
**
*
ns
ns
v-ATPase activity (uM phosphate)
0
2
4
Uninfected
WT
ΔSLO
HK
Strain